analytical chemistry

Article

pubs.acs.org/ac

# Amphipols Outperform Dodecylmaltoside Micelles in Stabilizing Membrane Protein Structure in the Gas Phase

Antonio N. Calabrese,[†] Thomas G. Watkinson,[†] Peter J. F. Henderson,[‡] Sheena E. Radford,[†] and Alison E. Ashcroft*[,†]

[†]School of Molecular and Cellular Biology and [‡]School of Biomedical Sciences, Astbury Centre for Structural Molecular Biology, University of Leeds, Leeds, LS2 9JT, United Kingdom

Supporting Information

**ABSTRACT:** Noncovalent mass spectrometry (MS) is emerging as an invaluable technique to probe the structure, interactions, and dynamics of membrane proteins (MPs). However, maintaining native-like MP conformations in the gas phase using detergent solubilized proteins is often challenging and may limit structural analysis. Amphipols, such as the well characterized A8-35, are alternative reagents able to maintain the solubility of MPs in detergent-free solution. In this work, the ability of A8-35 to retain the structural integrity of MPs for interrogation by electrospray ionization-ion mobility spectrometry-mass spectrometry (ESI-IMS-MS) is compared systematically with the commonly used detergent dodecylmaltoside. MPs from the two major structural classes were selected for analysis, including two $\beta$-barrel outer MPs, PagP and OmpT (20.2 and 33.5 kDa, respectively), and two $\alpha$-helical proteins, Mhp1 and GalP (54.6 and 51.7 kDa, respectively). Evaluation of the rotationally averaged collision cross sections of the observed ions revealed that the native structures of detergent solubilized MPs were not always retained in the gas phase, with both collapsed and unfolded species being detected. In contrast, ESI-IMS-MS analysis of the amphipol solubilized MPs studied resulted in charge state distributions consistent with less gas phase induced unfolding, and the presence of lowly charged ions which exhibit collision cross sections comparable with those calculated from high resolution structural data. The data demonstrate that A8-35 can be more effective than dodecylmaltoside at maintaining native MP structure and interactions in the gas phase, permitting noncovalent ESI-IMS-MS analysis of MPs from the two major structural classes, while gas phase dissociation from dodecylmaltoside micelles leads to significant gas phase unfolding, especially for the $\alpha$-helical MPs studied.

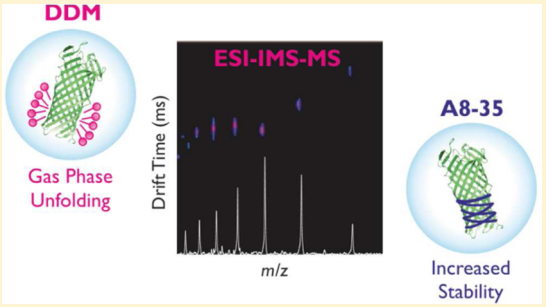


Membrane proteins (MPs) and their assemblies play vital roles in numerous biological processes and are common therapeutic targets.[1] Despite the fundamental role MPs play *in vivo*, their structural and functional characterization is hampered by their insolubility in aqueous solution, aggregation propensity, and difficulties in obtaining material in adequate quantities and of sufficient purity for analysis.[2] One major bottleneck of structural and functional studies of MPs is finding a suitable amphiphile that solubilizes and stabilizes the native protein structure for analysis.[3] To achieve this, detergents are commonly added above their critical micelle concentration (CMC) to MP-containing solutions. Detergent micelles, however, are a relatively poor membrane mimetic for many reasons, including their highly curved nature, relatively high monomeric concentrations (when compared with lipids), and altered lateral pressure.[4−6] As a result, many studies have demonstrated that solubilization of MPs with detergents may perturb their structure, influence their dynamics, or lead to aggregation.[5,7−11] Therefore, there is an urgent need to develop and utilize alternative methods of solubilization that maintain the structural and functional integrity of MPs for biochemical analysis.

As an alternative to detergent micelles, MPs can be solubilized by means of amphipathic polymers (amphipols, Apols) which function by interacting strongly with the surfaces of MPs via hydrophobic interactions.[12−14] The hydrophilic groups of the Apol maintain the solubility of the resultant complex. MP/Apol assemblies are highly stable, with the Apols having an extremely slow dissociation rate from the complex, resulting in increased MP stability in solution (e.g., bacteriorhodopsin has been shown to be stable for 7 days at 40 °C, while solubilization with detergent leads to protein aggregation within hours under these conditions).[12,13] There is an array of Apols with various structures, but the best characterized is the anionic A8-35 (Figure 1a), a polyacrylate polymer that is randomly grafted with octyl and isopropyl side chains.[15] Their structural diversity, general applicability, and novel properties have meant that Apols have been used to solubilize MPs for analysis using many structural techniques.[16−23]

**Received:** October 3, 2014
**Accepted:** December 13, 2014
**Published:** December 13, 2014

  

DOI: 10.1021/ac5037022
*Anal. Chem.* 2015, 87, 1118−1126

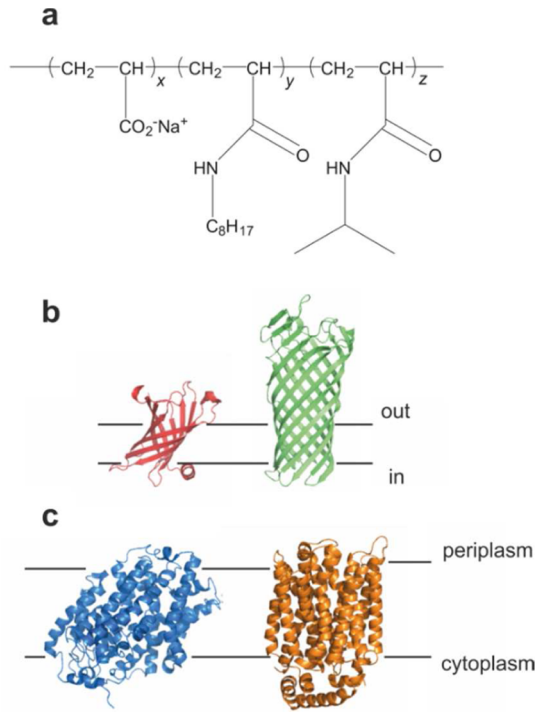


**Figure 1.** (a) The chemical structure of A8-35, which has an approximate mass of 4 kDa,[53] where $x$ = 29−34%, $y$ = 25−28%, and $z$ = 39−44%. (b) Crystal structures of PagP (left, PDB file 1THQ)[45] and OmpT (right, PDB file 1I78).[54] (c) Crystal structure of Mhp1 (left, PDB file 2X79),[55] and a homology model of GalP (right) based on the crystal structure of XylE which shares 30% sequence identity with GalP.[52]

Mass spectrometry (MS) is being employed increasingly for the study of MPs, with a variety of MS-based methods being developed for this purpose.[24−28] Noncovalent electrospray ionization (ESI)-MS, a technique that allows the native structure and noncovalent interactions of proteins to be retained in the gas phase, is especially valuable, particularly for determining the stoichiometry of MP assemblies, identifying bound species such as lipids, and gaining mechanistic insight into vital biological processes.[29−36] Coupling noncovalent ESI-MS with ion mobility spectrometry (IMS) allows the rotationally averaged collision cross sections (CCSs) of ions to be measured, together with their mass, in a single experiment,[37,38] which can afford information about the structure and dynamics of MPs.[39,40] To date, analysis of MPs by ESI-IMS-MS has relied on solubilization of the MP with detergents, with collisional activation of the MP/detergent complex *in vacuo* leading to release of the MP. However, it has been proposed that transitioning to detergent-free methods for the study of MPs by ESI-MS may lead to increased stabilization of MP structure in the gas phase, especially for proteins which require defined lipid environments.[41]

Several methods have been developed for the structural characterization of MPs by ESI-MS in the absence of detergent. MPs solubilized in amphipols, bicelles, and nanodiscs have been analyzed by ESI-MS,[41−44] with gas phase collisional activation leading to release of the MP from the assembly. Of these alternative solubilization methods, only MPs released from amphipols have been analyzed by ESI-IMS-MS,[42] but a systematic study of the differences in the ESI-IMS-MS spectra of MPs solubilized in either detergent or one of these alternative amphiphiles has not yet been reported. The one ground-breaking ESI-MS study that has been published to date proposed (based on charge state distributions) that more native-like conformers of MPs can be observed using amphipols, bicelles, and nanodiscs over detergents.[41] However, it remains uncertain if altering the solubilizing agent leads to differences in the conformational states of MPs in the gas phase and whether any general "rules" of which particular solubilizing agent is optimal for different MPs, or if each MP will behave differently, remain to be resolved.

In this work, we report, for the first time, a systematic comparison of the ESI-IMS-MS data of two very different structural classes of MPs solubilized either with detergent micelles of *n*-dodecyl-$\beta$-D-maltopyranoside (DDM) or with the Apol A8-35; furthermore, the solution phase and gas phase characteristics are compared. We chose for study the two $\beta$-barrel MPs, the acyl transferase PagP and the proteinase OmpT (Figure 1b),[42,45] together with the two all $\alpha$-helical MPs Mhp1,[46−48] a paradigm for the 5-helical inverted repeat transporter superfamily (5HIRT), and GalP,[49−51] a paradigm for the Major Facilitator Superfamily (MFS) (Figure 1c), as members of the two major structural classes of MP molecular architectures. High resolution structures (or in the case of GalP, a homology model based on the structure of XylE [30% identical in sequence])[52] of these four proteins are available, thus enabling a comparison of the measured CCSs with those estimated on the basis of these structures.

## METHODS

**OMP Expression and Purification.** $PagP_{his}$ and $OmpT_{his}$ were overexpressed in BL21 (DE3) *Escherichia coli* cells and isolated as inclusion bodies according to published protocols.[56,57] Briefly, cell pellets were resuspended in 50 mM Tris-HCl, 5 mM EDTA, pH 8.0, containing 1 mM PMSF and 2 mM benzamidine, and lysed by sonication. The lysate was pelleted by centrifugation (25 000*g*, 20 min, 4 °C), and the inclusion bodies were resuspended in 50 mM Tris-HCl, pH 8.0, and 2% (v/v) Triton X-100, stirred at room temperature for 1 h to permit solubilization of residual membranes, and then pelleted. The inclusion bodies were washed twice with 50 mM Tris-HCl, pH 8.0, with stirring and pelleting at each stage.

Purification of $PagP_{his}$ and $OmpT_{his}$ was achieved by means of $Ni^{2+}$-NTA affinity chromatography. The inclusion bodies were solubilized in denaturing buffer (10 mM Tris-HCl, pH 8.0, 250 mM NaCl, and 6 M guanidine hydrochloride, GuHCl) and filtered through a 0.22 $\mu$m syringe filter. The protein was bound to $Ni^{2+}$-NTA resin, and the resin washed with 10 mM Tris-HCl, pH 8.0, 250 mM NaCl, 6 M GuHCl, and 20 mM imidazole. $PagP_{his}$ or $OmpT_{his}$ were eluted with 10 mM Tris-HCl, pH 8.0, 250 mM NaCl, 6 M GuHCl, and 250 mM imidazole, and the protein was precipitated by overnight dialysis against deionized $H_2O$. The protein was stored as a precipitate at −20 °C.

Denatured $PagP_{his}$ and $OmpT_{his}$ were refolded by drop dilution into detergent-containing solution using previously published protocols.[58] Briefly, 1 mL of $PagP_{his}$ or $OmpT_{his}$ (5 $mg.mL^{-1}$) solubilized in 25 mM Tris-HCl and 6 M GuHCl, pH 8.0, was added dropwise to 20 mL of a stirring solution containing 10 mM Tris-HCl and 0.5% (w/v) *N*,*N*-dimethyldodecylamine *N*-oxide (LDAO), pH 8.0. The solution was incubated overnight with agitation at 4 °C. The solution was filtered through a 0.2 $\mu$m syringe filter and loaded onto a 1 mL HisTrap column (GE Healthcare, Little Chalfont, Bucks, U.K.) equilibrated with 10 mM Tris-HCl, pH 8.0, and 0.1% (w/v)


DOI: 10.1021/ac5037022
*Anal. Chem.* 2015, 87, 1118−1126

LDAO. A linear gradient over 10 column volumes was introduced to exchange the buffer to 10 mM Tris-HCl, pH 8.0, and 0.02% (w/v) DDM. The protein was eluted with 10 mM Tris-HCl, pH 8.0, 0.02% (w/v) DDM, and 200 mM imidazole, snap frozen, and stored at −80 °C.

**Cold SDS-PAGE.** Samples of either PagP or OmpT from folding reactions (10 μM) were mixed with 2× SDS-PAGE loading buffer [50 mM Tris−HCl, pH 6.8, 2% (w/v) SDS, 0.1% (w/v) bromophenol blue, and 10% (v/v) glycerol]. The samples were then immediately loaded onto a Tris−Tricine SDS-PAGE gel either prior to ("cold SDS-PAGE")[59] or after heating (95 °C for 5 min). Gels were stained using Instant Blue stain (Expedeon Ltd., Swavesey, Cambridge, UK). Folded and denatured/unfolded OMPs have different electrophoretic mobilities with native OMPs resisting unfolding by SDS in the absence of heat.[59] Separation of these states of the protein by cold SDS-PAGE permits their relative quantitation by densitometry analysis. This same behavior is not observed for α-helical MPs.

**Expression and Purification of Transport Proteins.** Mhp1 and GalP were expressed in *E. coli*, as previously described, using 100 L fermenters.[47,60] Cells were harvested using a continuous flow centrifuge, disrupted by explosive decompression, and the inner membranes were isolated by separation on a sucrose density gradient, before being stored at −80 °C.[47,60] The inner membranes were solubilized with 10 mM Tris-HCl, pH 8.0, 20 mM imidazole, 20% (v/v) glycerol, 300 mM NaCl, and 1% (w/v) DDM (60 mL) for 2 h at 4 °C with gentle agitation. The membranes were pelleted by ultracentrifugation (120 000*g*, 1 h, 4 °C), and the supernatant was mixed with 4 mL of Ni-NTA resin for 3 h at 4 °C with gentle agitation. The unbound material was removed, and the $Ni^{2+}$-NTA resin was washed with 10 mM Tris-HCl, pH 8.0, 20 mM imidazole, 10% (v/v) glycerol, and 0.05% (w/v) DDM. The protein was eluted from the resin with 10 mM Tris-HCl, pH 8.0, 200 mM imidazole, 2.5% (v/v) glycerol, and 0.05% (w/v) DDM. The eluate was analyzed by SDS-PAGE and Western blotting using the HisProbe-HRP antibody conjugate (Thermo Scientific, Hemel Hempstead, Herts., UK).

**Amphipol Trapping.** MPs were trapped in Apol by adding A8-35 (Affymetrix Ltd., High Wycombe, Bucks., U.K.) to detergent solubilized MPs in a 1:5 (w/w) ratio of MP/A8-35 and then incubating on ice for 30 min. The detergent was removed by incubating with BioBeads (Bio-Rad, Hemel Hempstead, Herts., UK) (20 g wet beads per g of detergent) for 1 h at 4 °C with gentle agitation. A8-35 trapped MPs were then dialyzed against 100 mM $NH_4HCO_3$, pH 8.0, at 4 °C for 24 h.

**Circular Dichroism.** Far-UV circular dichroism (CD) spectra were recorded on a Chirascan CD spectrophotometer (Applied Photophysics, Leatherhead, Surrey, UK) using a 0.1 mm path length cuvette. Spectra shown are the average of three scans that were acquired over the range of 200−260 nm with a bandwidth of 1 nm and a scan speed of 20 nm $min^{-1}$. The buffer contribution was subtracted from each sample. For the amphipol containing samples, buffer containing the appropriate amount of A8-35 was used as the reference.

**PagP Activity Assay.** An enzymatic assay for PagP activity was performed as previously described.[42,56] Briefly, *p*-nitrophenyl palmitate (p-NPP, 1 mM) was added (from a 10 mM solution in 2-propanol) to a solution of PagP (5 μM in 100 mM $NH_4HCO_3$, pH 8.0, supplemented with either 0.02% (w/v) DDM or 0.03 mg·$mL^{-1}$ A8-35). The hydrolysis of p-NPP to *p*-nitrophenol (p-NP) was monitored over 60 min by observing the increase in absorbance at 410 nm.

**OmpT Activity Assay.** The protease activity of OmpT was assessed by monitoring the time-dependent cleavage of a self-quenching fluorescent peptide (Abz-ARRAY-$NO_3$, Peptide Protein Research, Fareham, Hampshire, UK).[42,61] Cleavage of the peptide was detected as increased fluorescence at 430 nm following excitation at 325 nm using a QuantaMaster spectrofluorometer (Photon Technology International, Ford, West Sussex, UK). The fluorescence assay was initiated by addition of peptide (192 μM) to varying concentrations of folded OmpT (150 nM to 3.2 μM) in 100 mM $NH_4HCO_3$, pH 8.0, supplemented with either 1:5 (w/w) A8-35 or 0.02% (w/v) DDM. Samples were mixed manually, resulting in a dead time of 5−10 s. Assays were repeated in the presence or absence of 1 mg·$mL^{-1}$ lipopolysaccharide (LPS, Sigma-Aldrich, Gillingham, Dorset, UK). Specific activities were calculated from the initial rate in the increase of fluorescence, correcting for OmpT concentration, OmpT folding yield (judged by cold SDS-PAGE),[59] peptide concentration, and end point fluorescence (after 1 h). The mean activity for OmpT solubilized in either A8-35 or DDM was calculated from three repeats at four concentrations of OmpT ($n = 12$). OmpT specific activity units are displayed as mol(peptide cleaved)·$mol^{-1}$(OmpT)·$s^{-1}$ (eq 1). The specific activities of OmpT in A8-35 and DDM were significantly different as determined by an unpaired parametric *t* test ($p < 0.05$).

$$\text{specific activity} = \frac{\text{initial rate}}{\text{endpoint fluorescence}} \times \frac{[\text{substrate}]}{[\text{OmpT}]} \quad (1)$$

**Mhp1 and GalP Binding Assays.** The ability of DDM and A8-35 solubilized Mhp1 and GalP to bind known targets was assessed by fluorescence emission spectroscopy on a QuantaMaster spectrofluorometer (Photon Technology International, Ford, West Sussex, UK), using previously published methods.[47] Briefly, purified Mhp1 or GalP (200 μg/mL) solubilized in either 0.02% (w/v) DDM or by addition of a 1:5 (w/w) excess of A8-35 in 100 mM $NH_4HCO_3$, pH 8.0, were analyzed at 20 °C. Tryptophan fluorescence of protein samples was excited at 295 nm, and the intrinsic fluorescence emission at 330 nm was monitored. Micromolar additions of ligand (L-benzylhydantoin for Mhp1 and forskolin for GalP) were performed from 0 to 2 mM (Mhp1) or 0−100 μM (GalP). Samples were mixed for 1 min after each addition before measuring the fluorescence emission spectrum. Nonlinear regression analysis was performed using GraphPad Prism 6 (Graphpad Software, San Diego, CA, USA).

**Mass Spectrometry.** ESI-IMS-MS experiments were conducted on a Synapt HDMS mass spectrometer (Waters Ltd., Wilmslow, Manchester, UK). Nano-ESI was achieved using in-house manufactured gold-plated borosilicate capillaries. Typically, a capillary voltage of 1.7 kV was applied; the cone voltage was set to 80−150 V, and a backing pressure of 6−8 mbar was used. The bias voltage (20−80 V), as well as the voltages applied to the trap (50−100 V) and transfer (10−50 V) T-waves, were optimized to liberate the MP from the MP/Apol or MP/detergent complex while minimizing perturbations to the MP structure. IM separation was achieved by ramping the wave height from 5 to 30 V, at a speed of 300 $ms^{-1}$. Collision induced unfolding (CIU) experiments were conducted by increasing the Trap collision cell voltage in 5 V increments. Drift times were calibrated using experimentally


DOI: 10.1021/ac5037022
*Anal. Chem.* 2015, 87, 1118−1126

determined CCSs of native proteins and applying a procedure described in detail elsewhere.[37,38,62,63] CCSs were calculated from coordinates deposited in the Protein Data Bank, or from model structures, using a scaled projection approximation (PSA).[64] Aqueous CsI was used for $m/z$ calibration. Data were processed using MassLynx v4.1 and Driftscope v2.5 software (Waters Ltd., Wilmslow, Manchester, UK) employing IMS filtering.

## RESULTS AND DISCUSSION

**$\beta$-Barrel Outer Membrane Proteins PagP and OmpT.** Two $\beta$-barrel outer membrane proteins (OMPs), PagP and OmpT, were chosen for the study since these proteins have been shown previously to fold in A8-35 (both proteins also have crystal structures available for CCS estimation, required for comparison with MS data),[42,65] although a detailed characterization of the effects of MS and solution conditions on the gas phase structure and stability of these refolded proteins was not previously carried out nor compared with their behavior in detergent. PagP is an eight-stranded 20.2 kDa $\beta$-barrel OMP (Figure 1b) whose role *in vivo* is to transfer a palmitate chain from a phospholipid to lipid A.[45] The larger OmpT $\beta$-barrel comprises ten $\beta$-strands (33.5 kDa) (Figure 1b) and functions as an endopeptidase.[61]

Cold SDS-PAGE confirmed that PagP and OmpT are able to fold successfully (in excess of 80% yield, as determined by densitometry) in both DDM and A8-35-containing solutions, as the folded proteins migrate with an apparent lower molecular weight compared with the unfolded material (Figures S1a and S2a, Supporting Information).[59] Correct folding was also confirmed by circular dichroism (CD) with negative maxima at 218 nm for PagP and OmpT indicative of $\beta$-sheet structure in both DDM and A8-35 (Figures S1b,c and S2b,c, Supporting Information). CD spectra of PagP solubilized in DDM and A8-35 also have a characteristic maximum at 232 nm, as a result of the Cotton effect arising from close packing of residues Tyr26 and Trp66 (Figure S1b,c, Supporting Information).[58,66] In a previous study in which PagP was folded directly into A8-35 from its denatured state in 8 M urea, this characteristic feature was absent from the CD spectrum indicating that the final structure, while native-like, had subtle conformational perturbations.[42] The data presented herein show, in contrast, that introduction into A8-35 from a detergent-folded conformation results in native PagP which has the characteristic packing of aromatic residues in the core of the barrel. It should be noted that different folding mechanisms for PagP have also been observed elsewhere when folding into bilayers with different lipid compositions and at different lipid/protein ratios, indicating that folding can be influenced by solution conditions.[67]

PagP was confirmed to be enzymatically active when solubilized with both DDM and A8-35 by monitoring the time dependent increase in absorbance at 410 nm upon hydrolysis of *p*-nitrophenol palmitate (*p*-NPP) to *p*-nitrophenol (*p*-NP) (Figure S1d, Supporting Information).[56] The protease activity of OmpT was also assessed by monitoring the ability of the refolded protein to cleave a fluorogenic peptide (Abz-ARRAY-$NO_3$) (Figure S2d, Supporting Information). DDM and A8-35 solubilized OmpT were both inactive in the absence of LPS but displayed protease activity upon addition of this necessary cofactor.[61] However, the activities of the protein in the two amphiphiles are different, with the DDM solubilized protein having enhanced activity compared with the A8-35-trapped OmpT (Figure S2d, Supporting Information). Although ligand binding has been shown to be unaffected in many systems by A8-35, it has been proposed that conformational changes and interactions may be slowed.[12,68] The diminished OmpT activity in A8-35, therefore, may be a consequence of the restrictive, rigid nature of MP/A8-35 complexes, especially when compared with dynamic MP/detergent micelle structures.

ESI-IMS-MS analysis of the small OMP, PagP, revealed that the protein could be released from both DDM micelles and an A8-35 trapped state when collision energies as low as 60 V were applied in the Trap T-wave ion guide, resulting in spectra with similar charge state distributions (Figure 2a,b). Small quantities of DDM-adducted PagP could also be observed in the ESI-IMS-MS spectrum of PagP, as previously reported (Figure 2a).[65] Analysis of the CCSs of the observed ions indicates that the structure of PagP is largely retained in the gas phase irrespective of the amphiphile used to stabilize the MP in solution (Figure 2c). The measured CCSs of PagP at the lowest charge state observed (+5) were 1857 Å$^2$ in DDM and 1877 Å$^2$ in A8-35 (Table S1, Supporting Information). These CCSs are smaller than that expected for PagP based on its crystal structure (2290 Å$^2$)[65] and indicate that in both instances partial gas phase collapse, likely of loop regions, occurred, as has been reported previously.[65] At higher charge states, an unfolded population of PagP is observed, likely due to gas phase unfolding (Figure 2c).

The similar charge state distributions and CCSs observed for PagP in DDM and A8-35 led us to probe the gas phase stability of the protein solubilized in each amphiphile by performing collision-induced unfolding (CIU).[36,69] The Arrival Time Distributions (ATDs) of the 7+ ions of PagP at high energies have two features, corresponding to the collapsed structure and an unfolded conformation, but the unfolded conformation is absent at low energies (Figure 2d). CIU plots, which indicate the normalized ratio of the collapsed and unfolded conformations at various collision energies, are shown in Figure 2e for the 7+ ions of PagP solubilized with DDM or A8-35, respectively. These demonstrate that the A8-35 solubilized PagP unfolds at higher energies relative to the DDM solubilized protein. Thus, A8-35 has the ability to stabilize PagP against gas phase unfolding, increasing the lifetime of native-like structures in the gas phase reminiscent of the ability of A8-35 to stabilize MPs against unfolding and precipitation in solution.[12]

Liberation of OmpT from solutions in which the protein was solubilized in DDM or A8-35 could also be achieved by collisionally activating the solution-phase assemblies, with higher activation energies required to observe resolvable protein peaks (minimally 120 V in the Trap T-wave) than those used for PagP (Figure 3a). The ESI-IMS-MS spectra obtained are strikingly different, with lower charge state ions observed when OmpT is released from an A8-35 trapped state compared with the additional higher charged ions observed in DDM. A small amount of dimer is observed in the spectrum of DDM solubilized OmpT, due to self-association of OmpT in the urea free solution, as has been reported previously.[70] The calculation of CCSs from ATDs of liberated ions show both DDM and A8-35 are capable of maintaining native-like OmpT in the gas phase (Figure 3c,d). The most lowly charged OmpT ions have measured CCSs of 2741 Å$^2$ in DDM (7+ charge state) and 2722 Å$^2$ in A8-35 (5+ charge state). Both CCSs are approximately 8% smaller than that calculated from the crystal structure (3017 Å$^2$), suggesting that a degree of conformational


DOI: 10.1021/ac5037022
*Anal. Chem.* 2015, 87, 1118−1126

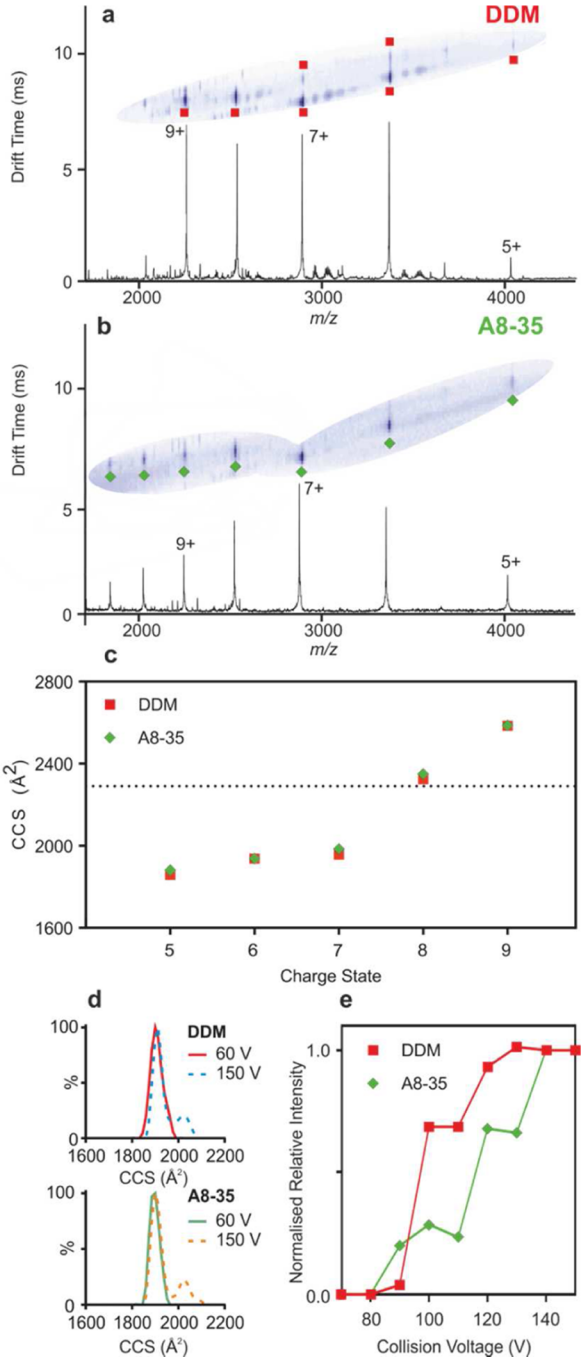


**Figure 2.** ESI-IMS-MS data for (a) DDM (red squares) and (b) A8-35 (green diamonds) solubilized PagP acquired under identical instrument parameters (Trap collision energy 100 V). (c) Experimentally determined CCSs of the observed ions at a collision energy of 80 V, with the expected value (based on calculations from the published crystal structure, PDB file 1THQ)[45] indicated by a dotted line. (d) ATDs of PagP (7+ charge state) in DDM and A8-35 at high (dashed lines) and low (solid lines) collision energies. (e) Collision-induced unfolding plot of PagP (7+ charge state) solubilized with DDM and A8-35.

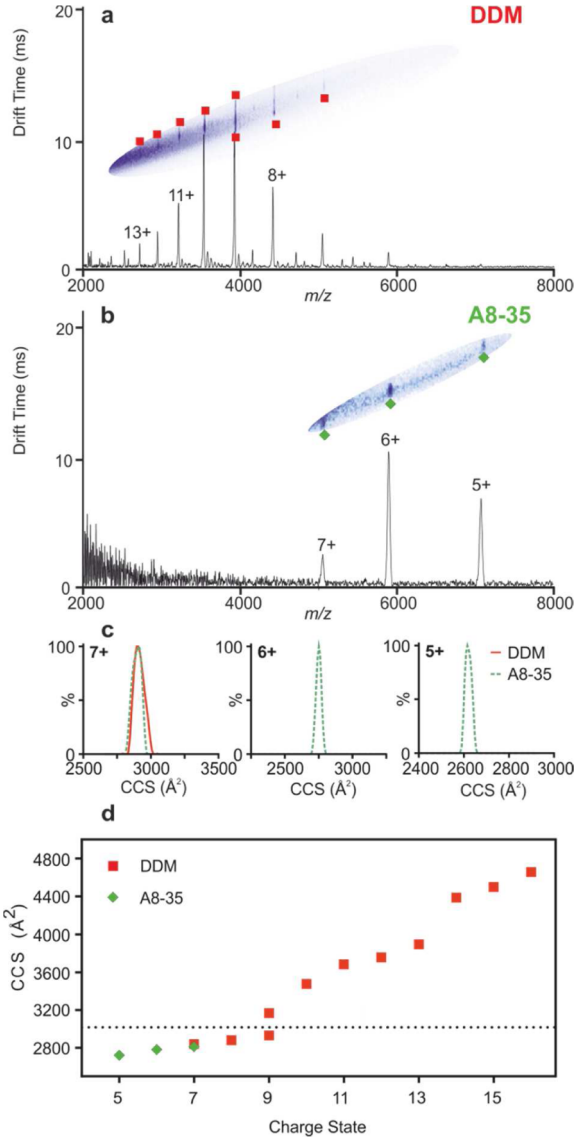


**Figure 3.** ESI-IMS-MS data for (a) DDM (red squares) and (b) A8-35 (green diamonds) solubilized OmpT acquired under identical instrument parameters (Trap collision energy 180 V). (c) ATDs for the three lowest observed charge states for DDM (solid red line) and A8-35 (dashed green line) solubilized OmpT. (d) Experimentally determined CCSs of the observed ions, with the value based on calculations from the published crystal structure, PDB file 1I78[54] indicated by a dotted line.

collapse is occurring in the gas phase, likely in loop regions of the structure, as has been observed for the $\beta$-barrels PagP (Figure 1) and OmpA.[54,71] Increasing the collision energy above that required to liberate the protein (up to 200 V in the Trap T-wave) and observe a resolved mass spectrum, did not result in a significant change in the CCS of the ions (Figure S3, Supporting Information). More expanded OmpT conformers (those with greater charge (10+ to 16+)) were observed when liberating the protein from DDM micelles, with the measured CCSs indicating that multiple conformations are present (Figure 3d). This is consistent with OmpT being prone to gas phase induced unfolding upon collisional activation of the OmpT/DDM complex. In contrast, activation of the OmpT/A8-35 assembly results only in lowly charged ions being observed and no ions which correspond to an unfolded population of conformations, demonstrating that A8-35 is more adept at stabilizing OmpT for ESI-IMS-MS analysis than DDM (even though analysis of both DDM and A8-35 solubilized OmpT leads to some gas phase collapse).

**$\alpha$-Helical Membrane-Embedded Transport Proteins Mhp1 and GalP.** To examine the ability of A8-35 to stabilize


DOI: 10.1021/ac5037022
*Anal. Chem.* 2015, 87, 1118−1126

MP structures in the gas phase further, we investigated two α-helical membrane transporters, Mhp1 and GalP (Figure 1c). Mhp1 is a 54.6 kDa $Na^+$ coupled hydantoin transporter and a member of the nucleobase-cation-symport 1 (NCS1) family of transporters which are involved in nucleobase salvage pathways and vitamin influx.[47,55] The 12 transmembrane helix bundle of Mhp1 undergoes significant conformational changes as it transports its substrate.[47,55] GalP is the 51.7 kDa galactose-$H^+$ symporter from *E. coli* and is a member of the major facilitator superfamily (MFS) of transport proteins.[72−74] There is limited structural information available for this protein[49] and other related members of the MFS; however, they are generally predicted to comprise 12 transmembrane helices, and structures have been proposed using homology modeling (Figure 1c).

CD was used to confirm that both Mhp1 and GalP are folded when solubilized with either DDM or A8-35, with each spectrum exhibiting a characteristic α-helical signal with negative maxima observed at 208 and 220 nm (Figures S4a,b and S5a,b, Supporting Information). Subtle differences in the relative intensities of the two negative maxima were observed in the CD spectra of the DDM solubilized and A8-35-trapped proteins, indicating that minor conformational variances may result depending on the amphiphile used. The activities of the DDM and A8-35 solubilized proteins were assessed using ligand binding assays monitored by tryptophan fluorescence quenching (see Methods). The activity of Mhp1 was evaluated by monitoring binding to L-benzylhydantoin, a known ligand, which binds in a $Na^+$-dependent fashion (Figure S4c,d, Supporting Information).[47,55] GalP activity was assessed by monitoring binding to the small molecule inhibitor forskolin (Figure S5c,d, Supporting Information).[75,76] Altering the amphiphile used to solubilize the protein did not significantly affect substrate binding, with similar $K_d$ values determined. Together, these data indicate that Mhp1 and GalP are both folded and functional when solubilized with either DDM or A8-35.

Analysis of DDM and A8-35 solubilized Mhp1 and GalP by use of ESI-IMS-MS resulted in peaks corresponding to each MP, as well as those originating from protein-bound lipids retained from the purification procedure (Figures 4a,c and 5a,c). Collision energies had to be set to much higher levels than for both of the OMPs (with the Trap T-wave collision energy having to be raised to 180 V) before resolvable protein peaks were observed. Both phosphatidylethanolamine (PE) and cardiolipin (CL) were identified by lipid extraction and further analysis by ESI-MS/MS in negative ion mode (data not shown), common components of the *E. coli* inner membrane from which the MPs were isolated.[77] In the case of the DDM solubilized proteins (Figures 4a,b and 5a,b), a narrow range of charge states was observed in the spectra. In contrast, a much broader range of charge state ions was observed in the ESI-IMS-MS spectra of A8-35 solubilized Mhp1 and GalP (Figures 4c,d and 5c,d), with more lowly charged species present, indicating the gas phase conformations of the proteins also contain more compact/folded species. Analysis of the measured CCSs of the observed ions reinforces this, with the lowly charged ions liberated from the A8-35 trapped protein samples having CCSs which indicate they are of relatively compact structure, unlike the ions observed upon analysis of the DDM solubilized protein (Figures 4e and 5e). The lowest observed charge state ions for A8-35 trapped Mhp1 (7+) had a measured CCS of 3916 $Å^2$, within 3.9% of the CCS predicted from the X-ray structure of the inward-open conformer of Mhp1 (3771 $Å^2$) (Table S1, Supporting Information). By comparison, the lowest charge state ions observed in DDM (12+) had an ATD with two features (Figure 4b), with the faster (or more compact) component having a CCS of 4939 $Å^2$, some 30% larger than predicted (Table S1, Supporting Information). Similarly, the lowest charge state ions observed for GalP (7+) had a

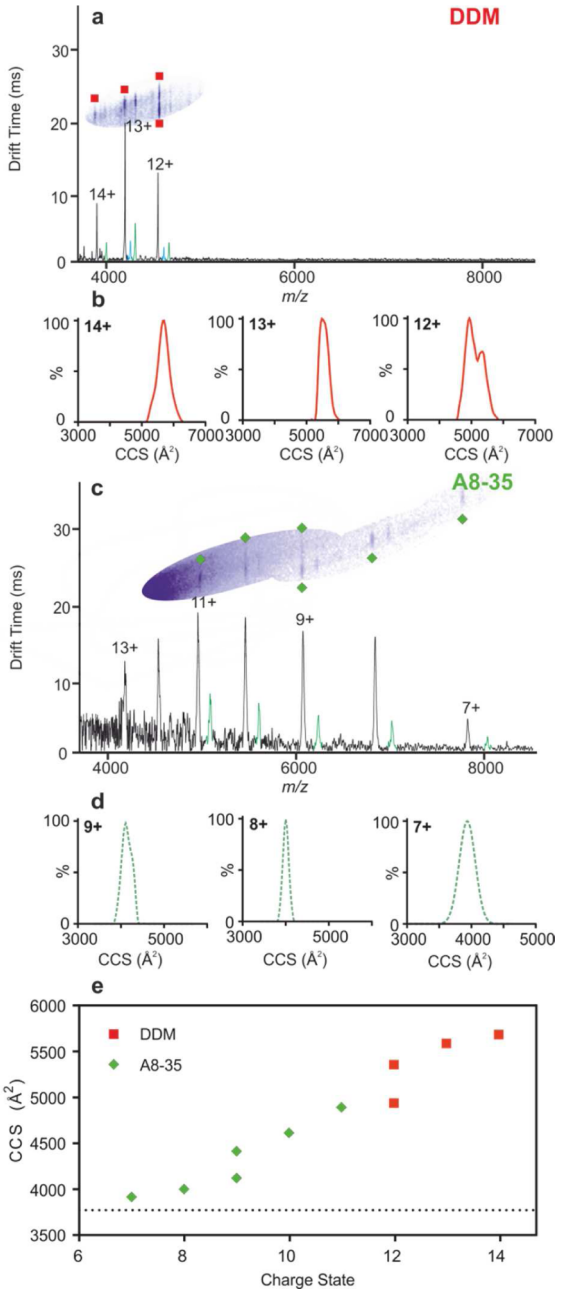


**Figure 4.** ESI-IMS-MS data for DDM and A8-35 solubilized Mhp1 acquired under identical instrument parameters (Trap collision energy 180 V). (a) ESI-IMS-MS spectrum for DDM solubilized Mhp1 (red squares) and (b) ATDs for the three lowest observed charge states (solid red lines). (c) ESI-IMS-MS spectrum for A8-35 solubilized Mhp1 (green diamonds) and (d) ATDs for the three lowest observed charge states (dashed green lines). Peaks corresponding to PE- and CL-bound protein are colored in blue and green, respectively. (e) Experimentally determined CCSs of the observed ions, with the value based on calculations from the published crystal structure, PDB file 2X79[55] indicated by a dotted line.


DOI: 10.1021/ac5037022
*Anal. Chem.* 2015, 87, 1118−1126

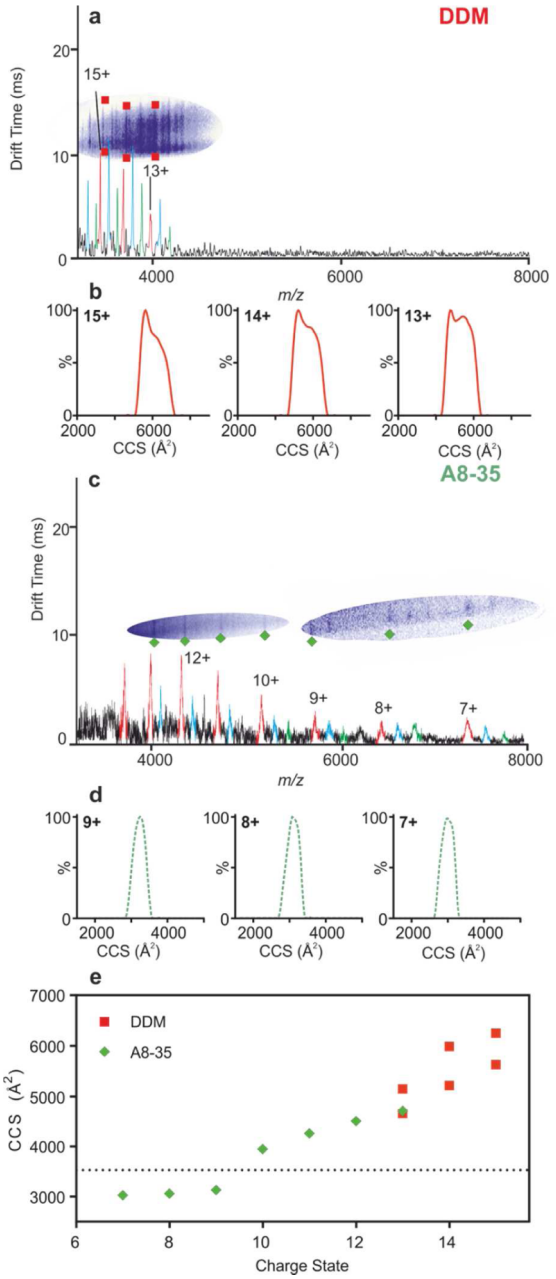


**Figure 5.** ESI-IMS-MS data for DDM and A8-35 solubilized GalP acquired under identical instrument parameters (Trap collision energy 180 V). (a) ESI-IMS-MS spectrum for DDM solubilized GalP (red peaks) and (b) ATDs for the three lowest observed charge states (solid red lines). (c) ESI-IMS-MS spectrum for A8-35 solubilized GalP (green diamonds) and (d) ATDs for the three lowest observed charge states (dashed green lines). Peaks corresponding to 2× PE- and 2× CL-bound protein are colored in blue and green, respectively. (e) Experimentally determined CCSs of the DDM (red squares) and A8-35 (green diamonds) solubilized observed GalP ions, with the value based on a model constructed from the published crystal structure of the homologous *E. coli* glucose transporter XylE[52] indicated by a dotted line.

measured CCS of 3028 Å$^2$, which was only present upon analysis of the A8-35 solubilized protein. This represents an approximately 15% difference with the CCS of the proposed model structure of GalP (3530 Å$^2$). The discrepancy between these two values could be attributed to the fact that this structure is modeled on the homologous protein XylE or could result from structural collapse occurring in loop regions in the gas phase. By comparison, all the charge state ions observed in DDM had ATDs with two features, with the lowest charge state (13+) having an ATD (Figure 5b) with a faster, more compact component having a CCS of 4657 Å$^2$, some 50% larger than the most compact conformer observed in the A8-35 solubilized sample (Table S1, Supporting Information).

## CONCLUSIONS

Application of noncovalent MS to probe the structure and function of MPs presents many challenges, primarily that the target must be solubilized with a suitable amphiphile which must be removed in the initial stages of the MS experiment to release the MP in the gas phase. To date, the addition of detergents has been the most common mechanism by which MPs are purified and solubilized for analysis by noncovalent MS,[32,36,41,78] and there is much evidence that this permits the retention of native structure in the gas phase. For example, molecular dynamics simulations have been used to demonstrate that DDM micelles protect gas phase structure of MPs,[79] and experimental evidence has shown that gas phase release of DDM from a MP/detergent micelle complex promotes the stabilization of a native structure.[65] The data presented here reinforce these observations, while further suggesting that these two phenomena may be dependent on the specific protein or protein complex under investigation, as well as the detergent used to solubilize the MP.[41]

It has been proposed that charging of proteins takes place upon entry into the gas phase[80] and that amphiphiles may protect the transmembrane regions of MPs from charging.[81] Here, we present the first systematic, comparative study of the behavior of $\alpha$-helical and $\beta$-sheet membrane proteins with both a detergent and an amphipol and compare gas phase results with solution phase behavior. Our data indicate that the amphipol A8-35 exerts a greater protective effect over the charging of MPs compared with DDM (as in general, ions with lower charge states were detected), which may be one reason why more native-like conformations are observed. These observations may be attributed to the dynamic nature of MP/detergent complexes, while A8-35 has been shown to bind to the transmembrane regions of MPs in a quasi-irreversible fashion.[12] In addition, amphipols have been shown to bind nonspecifically to MPs and to stabilize loop regions of MPs, in contrast with their interactions with detergents.[68,82] These additional contacts of A8-35 with the soluble regions of MPs may help to maintain their structural integrity upon collisional activation and energy dissipation from the MP/amphiphile by evaporative cooling upon release from A8-35.[83]

The strength of the MP/A8-35 interaction may also play a role in its ability to maintain native MP structures in the gas phase. It is proposed that detergent removal must take place rapidly enough to detect protein ions in the absence of bound detergent but not so fast as to expose the native protein structure to the harsh conditions of the collision cell for an extended period, as this may lead to unfolding or structural collapse.[83] The multiple contacts formed between a single A8-35 molecule and the transmembrane regions of MPs means that these interactions have very slow dissociation rates.[12] This property is fundamental to the ability of Apols to maintain native MP structure in solution but may also play a role in protecting the MP from unfolding in the gas phase.

In this work, we demonstrate that the four MPs studied, from two different structural families, are able to adopt native, active


DOI: 10.1021/ac5037022
*Anal. Chem.* 2015, 87, 1118−1126

structures in A8-35 and that native-like ions can be observed for all these MPs upon introduction into the gas phase from an A8-35 solubilized state. Added to the known advantages of Apols in maintaining the structural and functional integrity of MPs in solution for extended periods of time,[12] as well as the relative ease of either refolding or trapping MPs in Apols, this suggests that A8-35 solubilization coupled with ESI-IMS-MS presents an attractive means by which to characterize MPs from both structural classes. We also show that A8-35 solubilized MPs are transferred into the gas phase with lipid binding being maintained, thus permitting the study of MP/lipid interactions by ESI-IMS-MS, which is fundamentally important for attaining mechanistic insights into MP function.[36] The ability of Apols to maintain both the structural and functional integrity of MPs in both the gas and solution phases reinforces these novel amphiphiles as a valuable addition to the toolkit to probe MP structure using noncovalent MS techniques.

## ■ ASSOCIATED CONTENT

### Supporting Information

Additional information as noted in text. This material is available free of charge via the Internet at http://pubs.acs.org/.

## ■ AUTHOR INFORMATION


### Corresponding Author

*E-mail: a.e.ashcroft@leeds.ac.uk. Tel/Fax: +44(0) 113 343 7273.


### Notes

The authors declare no competing financial interest.

## ■ ACKNOWLEDGMENTS

We thank Dr. David J. Brockwell, Robert Schiffrin, and all members of the Ashcroft, Radford, and Henderson groups for helpful discussions. We also thank Prof. Jean-Luc Popot (CNRS, Paris, France) for helpful discussions regarding amphipols and Dr. Jocelyn Baldwin and Prof. Steven Baldwin for modelling the structure of GalP. We acknowledge David Sharples for his assistance with bacterial fermentation. The Biotechnology and Biological Sciences Research Council (BBSRC) is acknowledged for funding A.N.C. (BB/K000659/1) and T.G.W. (BB/K501827/1). The Synapt HDMS mass spectrometer was purchased with a Research Equipment Initiative grant from the BBSRC (BB/E012558/1), and the Chirascan CD spectrometer was purchased with funding from the Wellcome Trust (094232/Z/10/Z).

## ■ REFERENCES


(1) Almen, M. S.; Nordstrom, K. J.; Fredriksson, R.; Schioth, H. B. *BMC Biol.* **2009**, *7*, 50.

(2) Booth, P. J.; Templer, R. H.; Meijberg, W.; Allen, S. J.; Curran, A. R.; Lorch, M. *Crit. Rev. Biochem. Mol. Biol.* **2001**, *36*, 501−603.

(3) Warschawski, D. E.; Arnold, A. A.; Beaugrand, M.; Gravel, A.; Chartrand, E.; Marcotte, I. *Biochim. Biophys. Acta* **2011**, *1808*, 1957−1974.

(4) Garavito, R. M.; Ferguson-Miller, S. *J. Biol. Chem.* **2001**, *276*, 32403−32406.

(5) Cross, T. A.; Sharma, M.; Yi, M.; Zhou, H. X. *Trends Biochem. Sci.* **2011**, *36*, 117−125.

(6) Seddon, A. M.; Curnow, P.; Booth, P. J. *Biochim. Biophys. Acta* **2004**, *1666*, 105−117.

(7) Zoonens, M.; Comer, J.; Masscheleyn, S.; Pebay-Peyroula, E.; Chipot, C.; Miroux, B.; Dehez, F. *J. Am. Chem. Soc.* **2013**, *135*, 15174−15182.

(8) Lu, G. J.; Tian, Y.; Vora, N.; Marassi, F. M.; Opella, S. J. *J. Am. Chem. Soc.* **2013**, *135*, 9299−9302.

(9) Hong, H.; Bowie, J. U. *J. Am. Chem. Soc.* **2011**, *133*, 11389−11398.

(10) Zhou, H. X.; Cross, T. A. *Annu. Rev. Biophys.* **2013**, *42*, 361−392.

(11) Zhou, Y.; Lau, F. W.; Nauli, S.; Yang, D.; Bowie, J. U. *Protein Sci.* **2001**, *10*, 378−383.

(12) Popot, J. L.; Althoff, T.; Bagnard, D.; Baneres, J. L.; Bazzacco, P.; Billon-Denis, E.; Catoire, L. J.; Champeil, P.; Charvolin, D.; Cocco, M. J.; Cremel, G.; Dahmane, T.; de la Maza, L. M.; Ebel, C.; Gabel, F.; Giusti, F.; Gohon, Y.; Goormaghtigh, E.; Guittet, E.; Kleinschmidt, J. H.; Kuhlbrandt, W.; Le Bon, C.; Martinez, K. L.; Picard, M.; Pucci, B.; Sachs, J. N.; Tribet, C.; van Heijenoort, C.; Wien, F.; Zito, F.; Zoonens, M. *Annu. Rev. Biophys.* **2011**, *40*, 379−408.

(13) Popot, J. L. *Annu. Rev. Biochem.* **2010**, *79*, 737−775.

(14) Zoonens, M.; Popot, J. L. *J. Membr. Biol.* **2014**, *247*, 759−796.

(15) Tribet, C.; Audebert, R.; Popot, J. L. *Proc. Natl. Acad. Sci. U. S. A.* **1996**, *93*, 15047−15050.

(16) Gohon, Y.; Dahmane, T.; Ruigrok, R. W.; Schuck, P.; Charvolin, D.; Rappaport, F.; Timmins, P.; Engelman, D. M.; Tribet, C.; Popot, J. L.; Ebel, C. *Biophys. J.* **2008**, *94*, 3523−3537.

(17) Zoonens, M.; Giusti, F.; Zito, F.; Popot, J. L. *Biochemistry* **2007**, *46*, 10392−10404.

(18) Zoonens, M.; Catoire, L. J.; Giusti, F.; Popot, J. L. *Proc. Natl. Acad. Sci. U. S. A.* **2005**, *102*, 8893−8898.

(19) Catoire, L. J.; Damian, M.; Giusti, F.; Martin, A.; van Heijenoort, C.; Popot, J. L.; Guittet, E.; Baneres, J. L. *J. Am. Chem. Soc.* **2010**, *132*, 9049−9057.

(20) Catoire, L. J.; Zoonens, M.; van Heijenoort, C.; Giusti, F.; Popot, J. L.; Guittet, E. *J. Magn. Reson.* **2009**, *197*, 91−95.

(21) Cvetkov, T. L.; Huynh, K. W.; Cohen, M. R.; Moiseenkova-Bell, V. Y. *J. Biol. Chem.* **2011**, *286*, 38168−38176.

(22) Cao, E.; Liao, M.; Cheng, Y.; Julius, D. *Nature* **2013**, *504*, 113−118.

(23) Liao, M.; Cao, E.; Julius, D.; Cheng, Y. *Nature* **2013**, *504*, 107−112.

(24) Barrera, N. P.; Robinson, C. V. *Annu. Rev. Biochem.* **2011**, *80*, 247−271.

(25) Pan, Y.; Piyadasa, H.; O'Neil, J. D.; Konermann, L. *J. Mol. Biol.* **2012**, *416*, 400−413.

(26) Schmidt, C.; Robinson, C. V. *FEBS J.* **2014**, *281*, 1950−1964.

(27) Konermann, L.; Vahidi, S.; Sowole, M. A. *Anal. Chem.* **2014**, *86*, 213−232.

(28) Pan, Y.; Ruan, X.; Valvano, M. A.; Konermann, L. *J. Am. Soc. Mass Spectrom.* **2012**, *23*, 889−898.

(29) Housden, N. G.; Hopper, J. T.; Lukoyanova, N.; Rodriguez-Larrea, D.; Wojdyla, J. A.; Klein, A.; Kaminska, R.; Bayley, H.; Saibil, H. R.; Robinson, C. V.; Kleanthous, C. *Science* **2013**, *340*, 1570−1574.

(30) Marcoux, J.; Wang, S. C.; Politis, A.; Reading, E.; Ma, J.; Biggin, P. C.; Zhou, M.; Tao, H.; Zhang, Q.; Chang, G.; Morgner, N.; Robinson, C. V. *Proc. Natl. Acad. Sci. U. S. A.* **2013**, *110*, 9704−9709.

(31) Zhou, M.; Morgner, N.; Barrera, N. P.; Politis, A.; Isaacson, S. C.; Matak-Vinkovic, D.; Murata, T.; Bernal, R. A.; Stock, D.; Robinson, C. V. *Science* **2011**, *334*, 380−385.

(32) Laganowsky, A.; Reading, E.; Hopper, J. T.; Robinson, C. V. *Nat. Protoc.* **2013**, *8*, 639−651.

(33) Barrera, N. P.; Isaacson, S. C.; Zhou, M.; Bavro, V. N.; Welch, A.; Schaedler, T. A.; Seeger, M. A.; Miguel, R. N.; Korkhov, V. M.; van Veen, H. W.; Venter, H.; Walmsley, A. R.; Tate, C. G.; Robinson, C. V. *Nat. Methods* **2009**, *6*, 585−587.

(34) Barrera, N. P.; Zhou, M.; Robinson, C. V. *Trends Cell Biol.* **2013**, *23*, 1−8.

(35) Schmidt, C.; Zhou, M.; Marriott, H.; Morgner, N.; Politis, A.; Robinson, C. V. *Nat. Commun.* **2013**, *4*, 1985.

(36) Laganowsky, A.; Reading, E.; Allison, T. M.; Ulmschneider, M. B.; Degiacomi, M. T.; Baldwin, A. J.; Robinson, C. V. *Nature* **2014**, *510*, 172−175.




DOI: 10.1021/ac5037022
*Anal. Chem.* 2015, 87, 1118−1126

(37) Ruotolo, B. T.; Benesch, J. L. P.; Sandercock, A. M.; Hyung, S.-J.; Robinson, C. V. *Nat. Protoc.* **2008**, *3*, 1139−1152.
(38) Smith, D. P.; Knapman, T. W.; Campuzano, I.; Malham, R. W.; Berryman, J. T.; Radford, S. E.; Ashcroft, A. E. *Eur. J. Mass Spectrom.* **2009**, *15*, 113−130.
(39) Wang, S. C.; Politis, A.; Di Bartolo, N.; Bavro, V. N.; Tucker, S. J.; Booth, P. J.; Barrera, N. P.; Robinson, C. V. *J. Am. Chem. Soc.* **2010**, *132*, 15468−15470.
(40) Zhou, M.; Politis, A.; Davies, R. B.; Liko, I.; Wu, K. J.; Stewart, A. G.; Stock, D.; Robinson, C. V. *Nat. Chem.* **2014**, *6*, 208−215.
(41) Hopper, J. T. S.; Yu, Y. T.-C.; Li, D.; Raymond, A.; Bostock, M.; Liko, I.; Mikhailov, V.; Laganowsky, A.; Benesch, J. L. P.; Caffrey, M.; Nietlispach, D.; Robinson, C. V. *Nat. Methods* **2013**, 1−6.
(42) Leney, A. C.; McMorran, L. M.; Radford, S. E.; Ashcroft, A. E. *Anal. Chem.* **2012**, *84*, 9841−9847.
(43) Marty, M. T.; Zhang, H.; Cui, W.; Gross, M. L.; Sligar, S. G. *J. Am. Soc. Mass Spectrom.* **2014**, *25*, 269−277.
(44) Marty, M. T.; Zhang, H.; Cui, W.; Blankenship, R. E.; Gross, M. L.; Sligar, S. G. *Anal. Chem.* **2012**, *84*, 8957−8960.
(45) Ahn, V. E.; Lo, E. I.; Engel, C. K.; Chen, L.; Hwang, P. M.; Kay, L. E.; Bishop, R. E.; Prive, G. G. *EMBO J.* **2004**, *23*, 2931−2941.
(46) Suzuki, S.; Henderson, P. J. F. *J. Bacteriol.* **2006**, *188*, 3329−3336.
(47) Weyand, S.; Shimamura, T.; Yajima, S.; Suzuki, S.; Mirza, O.; Krusong, K.; Carpenter, E. P.; Rutherford, N. G.; Hadden, J. M.; O'Reilly, J.; Ma, P.; Saidijam, M.; Patching, S. G.; Hope, R. J.; Norbertczak, H. T.; Roach, P. C.; Iwata, S.; Henderson, P. J.; Cameron, A. D. *Science* **2008**, *322*, 709−713.
(48) Simmons, K. J.; Jackson, S. M.; Brueckner, F.; Patching, S. G.; Beckstein, O.; Ivanova, E.; Geng, T.; Weyand, S.; Drew, D.; Lanigan, J.; Sharples, D. J.; Sansom, M. S.; Iwata, S.; Fishwick, C. W.; Johnson, A. P.; Cameron, A. D.; Henderson, P. J. *EMBO J.* **2014**, *33*, 1831−1844.
(49) Jones, L. N.; Baldwin, S. A.; Henderson, P. J. F.; Ashcroft, A. E. *Rapid Commun. Mass Spectrom.* **2010**, *24*, 276−284.
(50) Venter, H.; Ashcroft, A. E.; Keen, J. N.; Henderson, P. J.; Herbert, R. B. *Biochem. J.* **2002**, *363*, 243−252.
(51) Findlay, H. E.; Rutherford, N. G.; Henderson, P. J.; Booth, P. J. *Proc. Natl. Acad. Sci. U. S. A.* **2010**, *107*, 18451−18456.
(52) Sun, L.; Zeng, X.; Yan, C.; Sun, X.; Gong, X.; Rao, Y.; Yan, N. *Nature* **2012**, *490*, 361−366.
(53) Giusti, F.; Rieger, J.; Catoire, L. J.; Qian, S.; Calabrese, A. N.; Watkinson, T. G.; Casiraghi, M.; Radford, S. E.; Ashcroft, A. E.; Popot, J. L. *J. Membr. Biol.* **2014**, *247*, 909−924.
(54) Vandeputte-Rutten, L.; Kramer, R. A.; Kroon, J.; Dekker, N.; Egmond, M. R.; Gros, P. *EMBO J.* **2001**, *20*, 5033−5039.
(55) Shimamura, T.; Weyand, S.; Beckstein, O.; Rutherford, N. G.; Hadden, J. M.; Sharples, D.; Sansom, M. S.; Iwata, S.; Henderson, P. J.; Cameron, A. D. *Science* **2010**, *328*, 470−473.
(56) Huysmans, G. H. M.; Radford, S. E.; Brockwell, D. J.; Baldwin, S. A. *J. Mol. Biol.* **2007**, *373*, 529−540.
(57) Burgess, N. K.; Dao, T. P.; Stanley, A. M.; Fleming, K. G. *J. Biol. Chem.* **2008**, *283*, 26748−26758.
(58) Khan, M. A.; Neale, C.; Michaux, C.; Pomes, R.; Prive, G. G.; Woody, R. W.; Bishop, R. E. *Biochemistry* **2007**, *46*, 4565−4579.
(59) Schnaitman, C. A. *Arch. Biochem. Biophys.* **1973**, *157*, 541−552.
(60) Weyand, S.; Ma, P.; Saidijam, M.; Baldwin, J.; Beckstein, O.; Jackson, S.; Suzuki, S.; Patching, S. G.; Shimamura, T.; Sansom, M. S. P.; Iwata, S.; Cameron, A. D.; Baldwin, S. A.; Henderson, P. J. F. In *Handbook of Metalloproteins*; Messerschmidt, A., Ed.; John Wiley: Chichester, 2010.
(61) Kramer, R. A.; Zandwijken, D.; Egmond, M. R.; Dekker, N. *Eur. J. Biochem.* **2000**, *267*, 885−893.
(62) Knapman, T. W.; Berryman, J. T.; Campuzano, I.; Harris, S. A.; Ashcroft, A. E. *Int. J. Mass Spectrom.* **2010**, *298*, 17−23.
(63) Bush, M. F.; Hall, Z.; Giles, K.; Hoyes, J.; Robinson, C. V.; Ruotolo, B. T. *Anal. Chem.* **2010**, *82*, 9557−9565.
(64) Bleiholder, C.; Wyttenbach, T.; Bowers, M. T. *Int. J. Mass Spectrom.* **2011**, *308*, 1−10.
(65) Borysik, A. J.; Hewitt, D. J.; Robinson, C. V. *J. Am. Chem. Soc.* **2013**, *135*, 6078−6083.
(66) Cuesta-Seijo, J. A.; Neale, C.; Khan, M. A.; Moktar, J.; Tran, C. D.; Bishop, R. E.; Pomes, R.; Prive, G. G. *Structure* **2010**, *18*, 1210−1219.
(67) Huysmans, G. H. M.; Radford, S. E.; Baldwin, S. A.; Brockwell, D. J. *J. Mol. Biol.* **2012**, *416*, 453−464.
(68) Perlmutter, J. D.; Popot, J. L.; Sachs, J. N. *J. Membr. Biol.* **2014**, *247*, 883−895.
(69) Hyung, S. J.; Robinson, C. V.; Ruotolo, B. T. *Chem. Biol.* **2009**, *16*, 382−390.
(70) Ebie Tan, A.; Burgess, N. K.; DeAndrade, D. S.; Marold, J. D.; Fleming, K. G. *Macromol. Biosci.* **2010**, *10*, 763−767.
(71) Marcoux, J.; Politis, A.; Rinehart, D.; Marshall, D. P.; Wallace, M. I.; Tamm, L. K.; Robinson, C. V. *Structure* **2014**, *22*, 781−790.
(72) Henderson, P. J.; Giddens, R. A.; Jones-Mortimer, M. C. *Biochem. J.* **1977**, *162*, 309−320.
(73) Baldwin, S. A.; Henderson, P. J. F. *Annu. Rev. Physiol.* **1989**, *51*, 459−471.
(74) Macpherson, A. J. S.; Jonesmortimer, M. C.; Horne, P.; Henderson, P. J. F. *J. Biol. Chem.* **1983**, *258*, 4390−4396.
(75) Martin, G. E. M.; Seamon, K. B.; Brown, F. M.; Shanahan, M. F.; Roberts, P. E.; Henderson, P. J. F. *J. Biol. Chem.* **1994**, *269*, 24870−24877.
(76) Martin, G. E. M.; Rutherford, N. G.; Henderson, P. J. F.; Walmsley, A. R. *Biochem. J.* **1995**, *308*, 261−268.
(77) Wessel, D.; Flugge, U. I. *Anal. Biochem.* **1984**, *138*, 141−143.
(78) Barrera, N. P.; Di Bartolo, N.; Booth, P. J.; Robinson, C. V. *Science* **2008**, *321*, 243−246.
(79) Rouse, S. L.; Marcoux, J.; Robinson, C. V.; Sansom, M. S. *Biophys. J.* **2013**, *105*, 648−656.
(80) Hogan, C. J., Jr.; Carroll, J. A.; Rohrs, H. W.; Biswas, P.; Gross, M. L. *J. Am. Chem. Soc.* **2008**, *130*, 6926−6927.
(81) Barrera, N. P.; Zhou, M.; Robinson, C. V. *Trends Cell Biol.* **2013**, *23*, 1−8.
(82) Etzkorn, M.; Raschle, T.; Hagn, F.; Gelev, V.; Rice, A. J.; Walz, T.; Wagner, G. *Structure* **2013**, *21*, 394−401.
(83) Borysik, A. J.; Robinson, C. V. *Phys. Chem. Chem. Phys.* **2012**, *14*, 14439−14449.


DOI: 10.1021/ac5037022
*Anal. Chem.* 2015, 87, 1118−1126